Incremental air-bending forming simulation of sheet metal based on anisotropic plasticity theory

ZEMIN FU*, DACHAO HU, XUHUI LIU
School of Mechanical Engineering, Shanghai Institute of Technology, Shanghai, P.R. China

Modeling of multiple-step incremental air-bending forming processes requires an accurate description of anisotropic material behavior. This paper describes the finite element (FE) simulation results obtained using Hill's quadratic anisotropic yield function under the conditions of plane stress and plane strain, respectively. The single-step air-bending and semiellipse-shaped workpiece multiple-step air-bending tests were modeled for WELDOX700, WELDOX900 and OPTIM960 anisotropic sheets, using the improved Hill's yield function embedded into ABAQUS. Then, the air-bending springback, thickness strain along the transverse direction and parts profiles were computed. The studies show that the results predicted with Hill's yielding criterion under the plane strain condition are in much better agreement with experiment data than those predicted with Hill's yielding criterion under the plane stress condition. It can be taken as a valuable mathematical tool used for multiple-step incremental air-bending forming simulation of anisotropic sheet metals.

(Received October 25, 2011; accepted November 23, 2011)

Keywords: Air-bending, Sheet metal incremental forming, Anisotropic material constitutive model, Finite element simulation

1. Introduction

Sheet metal multiple-step incremental air-bending forming process is a flexible sheet-metal-forming technology that uses principles of stepped manufacturing. It transforms the complicated geometry information into a series of parameters of single-step, and then the plastic deformation is carried out step by step through the computer numerical controlled movements of the punch and sheet feed for getting the desired part [1]. Therefore, the process is cost-effective to form large complex parts in small to medium batches, such as semiellipse-shaped workpieces with super length and large opening, which could be used as crane boom, telescopic arm of the concrete pump truck, boom of bridge, and petroleum piping, etc.

Incremental air-bending forming process generally involves large deformations and rotates which are both nonlinear with respect to material and geometry positions, respectively. So multiple-step incremental air-bending forming process is a nonlinear one. It could not be solved by quantitative mathematical analysis method. Trial-and-error methods are still being used to establish suitable procedures for multiple-step air-bending forming of sheet metal. Therefore, this study attempts to simulate multiple-step incremental air-bending forming with FEM and check its applicability from the view point of making the production process more efficient.

It should be noted that an acceptable material model in the FE simulation of sheet metal forming should be able to capture many different phenomena that occur during plastic deformation, such as the anisotropic yielding behavior, the proper strain-(or work-) hardening regime, etc. Anisotropy is closely related to the formability of material and should be considered carefully for the accurate analysis of sheet metal forming processes. Thus, the computer simulation codes, based on the finite element method that are widely used to design sheet forming, require accurate and numerically efficient anisotropic elasto-plastic constitutive models. Realistic constitutive description of sheet material requires a yield function that describes simultaneously anisotropy of yielding and anisotropy of plastic flow. To describe plastic anisotropy of rolled metal sheets, Hill (1948, 1950) developed a quadratic yield criterion by generalizing the classical Von Mises isotropic criterion to orthotropy [2-3]. Hill (1948) quadratic function is the most frequently used orthotropic yield function due to its simple functional form and the fact that its anisotropy parameters can be related to material properties explicitly in a simple manner. In Hill (1948) formulation, sheet material is described by four material parameters. Due to considering and analyzing uniaxial tensile properties of forming sheet material, this function is able to capture simultaneously anisotropy of yielding and anisotropy of strain ratios with acceptable accuracy. To capture the behaviour of various sheet materials in recent decades, many other anisotropic yield models have been developed, such as Hill (1979, 1990, 1993) [4-6], Barlat (1989, 1991, 1997, 2003) [7-11], Karafillis (1993) [12], et al. Some of these anisotropic plasticity models are able to describe the anisotropic behavior of sheet metals with considerable accuracy, but

they necessitate a large number of experiments to define the coefficients.

Both the forming and subsequent springback stages of the Numisheet's 96 Benchmark (S-type guide rail) were simulated with Hill'48 and Barlat'89 yielding criteria respectively [13]. The predictions of two different yield functions were compared with the experiment data, the results showed that Hill'48 anisotropic yield criterion was better able to describe the steel sheet material ($\bar{r}>1$, $\bar{r}$: anisotropy coefficient) yield behavior, while Barlat'89 anisotropic yield criterion could provide favorable agreement with the experimental value of sheet materials ($\bar{r}<1$, such as aluminum alloy) forming. Thus, Hill's quadratic yield criterion is very suitable for steel sheet forming [2], and Barlat's yield criterion is more adapt to aluminum alloy sheet forming [7]. Therefore, this research intends to simulate multiple-step incremental air-bending forming processes of sheet metal with Hill's quadratic yield criterion.

Numerous fundamental studies have been conducted over the years in an attempt to simulate sheet metal forming based on anisotropic elasto-plastic constitutive model [7, 14-19]. However, these researches are only limited to sheet metal forming under plane-stress conditions, relatively little has been devoted to the detailed analysis on the numerical simulation of sheet metal forming under plane-strain conditions. In order to effectively simulate the practical forming process for multiple-step incremental air-bending of anisotropic sheet metal, the authors think that it is of great value to simulate multiple-step incremental air-bending forming under the conditions of plane stress and plane strain respectively to obtain the optimized process parameters of large workpiece forming.

In this paper, the FE simulation is done by ABAQUS/Explicit & Standard solvers. Plane stress element CPS8R (namely the eight-node biquadratic plane stress quadrilateral, reduced integration shell elements) and plane strain element CPE8R (namely the eight-node biquadratic plane strain quadrilateral, reduced integration shell elements), elasto-plastic constitutive model based on Hill's (1948) quadratic anisotropic yield function are applied to simulate sheet metal multiple-step incremental air-bending forming processes respectively.. In Hill's yield function, anisotropy was defined with the yield stress ratios and the $\bar{r}$ -values in different orientations with respect to the rolling direction for the yield and potential functions, respectively. Then, the shape of the workpiece profile and the thickness strain along the transverse direction of workpiece, predicted with Hill's anisotropic material model under the plane stress and the plane strain embedded into ABAQUS, are compared with the experimental data to assess their abilities to improve the results of finite element simulatios. Finally, a large workpiece is manufactured with the optimized simulation results. Details of methods are given in the following sections.

2. Anisotropic elasto-plastic constitutive model

2.1 Hill's yield function for anisotropic sheets under plane stress conditions

In the developed model, the functional form of the yield function of Hill (1948) is used for yield function and plastic potential function. In sheet metal multiple-step incremental air-bending forming processes, sheet is subjected to the plane stress loading conditions. Thus, utilized functions are considered as functions of the in-plane stresses σ_{xx}, σ_{yy}, σ_{xy}, σ_{yx}, where x-axis denotes the original rolling direction of the sheet, while the y-axis denotes the sheet transverse direction, the z-axis denotes the sheet normal direction.

For plane stress conditions, the out-of-plane normal is zero ($\sigma_{zz}=0$). Stress and strain tensors (σ and ε) are stored in vector form there for the sake of simplicity and efficiently:

$$[\sigma]=[\sigma_{xx}\ \sigma_{yy}\ \sigma_{xy}]^T \tag{1}$$

$$[\varepsilon]=[\varepsilon_{xx}\ \varepsilon_{yy}\ \gamma_{xy}(=2\varepsilon_{xy})]^T \tag{2}$$

Due to $\sigma_{zz}=0$, The yield condition of Hill's quadratic yielding function for anisotropic sheets, by neglecting the higher order terms, can be expressed as:

$$f(\sigma_{ij},\varepsilon_{ij})=\sigma_{xx}^2+\sigma_{yy}^2-\frac{2\bar{r}}{1+\bar{r}}\sigma_{xx}\sigma_{yy}-\overline{\sigma}_e^{\,2}=0 \tag{3}$$

$$\bar{r}=\frac{r_0+2r_{45}+r_{90}}{4} \tag{4}$$

Where $\overline{\sigma}_e$ is equivalent stress; $\bar{r}$ is the normal anisotropy coefficient; ψ is yielding function; r_0, r_{45} and r_{90} denote the value of r at 0°, 45° and 90° with respect to the rolling direction of the sheet.

The constraint $\sigma_{zz}=0$ and the evolution equation for the plastic strains lead to:

$$\varepsilon_{zz}^e=\frac{-\nu}{(1-\nu)(\varepsilon_{xx}^e+\varepsilon_{yy}^e)} \tag{5}$$

$$\varepsilon_{zz}^p=-(\varepsilon_{xx}^p+\varepsilon_{yy}^p) \tag{6}$$

Where ν is Poisson's ratio.

Therefore, the strain $\varepsilon_{zz}=\varepsilon_{zz}^{e}+\varepsilon_{zz}^{p}$ is obtained if the plastic strains ε_{xx}^{p}, ε_{yy}^{p} and the stresses σ_{xx} and σ_{yy} are known:

$$\varepsilon_{zz}=\frac{-1}{1-\nu}\left(\frac{\nu}{\varepsilon_{xx}+\varepsilon_{yy}}+\frac{1-2\nu}{\varepsilon_{xx}^{p}+\varepsilon_{yy}^{p}}\right) \tag{7}$$

Considering plane-stress conditions, quadratic Hill (1948) yield function becomes:

$$f_y=(\lambda_{1y}\sigma_{xx}^{2}+\lambda_{2y}\sigma_{yy}^{2}-2j_y\sigma_{xx}\sigma_{yy}+\rho_y(\sigma_{xy}^{2}+\sigma_{yx}^{2}))^{\frac{1}{2}} \tag{8}$$

λ_{1y}, λ_{2y}, j_y and ρ_y are constant characteristics of the anisotropy and for the current anisotropic yield function are adjusted yield stresses:

$$\begin{aligned}
2(\lambda_{1y}-j_y)&=\sigma_{xx}^{2}\left(\frac{1}{\sigma_{xx}^{2}}-\frac{1}{\sigma_{yy}^{2}}+\frac{1}{\sigma_b^{2}}\right)\\
2(\lambda_{2y}-j_y)&=\sigma_{xx}^{2}\left(\frac{1}{\sigma_{yy}^{2}}-\frac{1}{\sigma_{xx}^{2}}+\frac{1}{\sigma_b^{2}}\right)\\
2j_y&=\sigma_{xx}^{2}\left(\frac{1}{\sigma_{xx}^{2}}+\frac{1}{\sigma_{yy}^{2}}-\frac{1}{\sigma_b^{2}}\right)\\
2\rho_y&=\sigma_{xx}^{2}\left(\frac{4}{\sigma_{45}^{2}}-\frac{1}{\sigma_b^{2}}\right)
\end{aligned} \tag{9}$$

The above are simplified as:

$$\lambda_{1y}=1,\ \lambda_{2y}=\left(\frac{\sigma_{xx}}{\sigma_{yy}}\right)^{2},\ j_y=0.5\left(1+\left(\frac{\sigma_{xx}}{\sigma_{yy}}\right)^{2}+\left(\frac{\sigma_{xx}}{\sigma_b}\right)^{2}\right),$$

$$\rho_y=2\left(\frac{\sigma_{xx}}{\sigma_{yy}}\right)^{2}-0.5\left(\frac{\sigma_{xx}}{\sigma_b}\right)^{2} \tag{10}$$

Where σ_{xx}, σ_{yy} and σ_{45} are tensile yield stresses in the rolling, transverse and diagonal (45), directions, σ_b is the equibiaxial yield stress.

By using the ratio of plastic strain increments to define the three r-values in different orientations relative to the rolling direction (r_0, r_{45} and r_{90}), we have:

$$\left.\begin{aligned}
r_0&=\frac{j_y}{\lambda_{1y}-\gamma_y}\\
r_{90}&=\frac{j_y}{\lambda_{2y}-j_y}\\
r_{45}&=\frac{1}{2}\left(\frac{2\rho_y}{\lambda_{1y}+\lambda_{2y}-2j_y}-1\right)
\end{aligned}\right\} \tag{11}$$

Plastic potential function with functional form identical as yield function defined by Eq.(8) reads:

$$f_p=(\lambda_{1p}\sigma_{xx}^{2}+\lambda_{2p}\sigma_{yy}^{2}-2j_p\sigma_{xx}\sigma_{yy}+\rho_p(\sigma_{xy}^{2}+\sigma_{yx}^{2}))^{\frac{1}{2}} \tag{12}$$

In which the new set of anisotropy coefficients, λ_{1p}, λ_{2p}, j_p and ρ_p, are dimensionless functions of the plastic strain ratios defined as follows:

$$\lambda_{1p}=1,\ \lambda_{2p}=\frac{1+1/r_{90}}{1+1/r_0},\ j_p=\frac{1}{1+1/r_0},$$

$$\rho_p=\frac{(1+2r_{45})(1/r_0+1/r_{90})}{2(1+1/r_0)} \tag{13}$$

The plastic potential function can also be written as:

$$f_p=\left(\frac{3}{2}\sigma^{T}Q\sigma\right)^{\frac{1}{2}} \tag{14}$$

Where [Q] is the potential function anisotropic tensor and is defined as:

$$[Q]=\begin{bmatrix} Q_1+Q_2 & -Q_1 & 0\\ -Q_1 & Q_1+Q_3 & 0\\ 0 & 0 & 2Q_4 \end{bmatrix} \tag{15}$$

Where $Q_1=\frac{2}{3}j_p$, $Q_2=\frac{2}{3}(\lambda_{1p}-j_p)$, $Q_3=\frac{2}{3}(\lambda_{2p}-j_p)$, and $Q_1=\frac{2}{3}\rho_p$.

Obviously, it can be seen that this model has the capability to describe both experimental aspects of anisotropy: yield stresses and plastic strain ratios. At the same time, the yield and plastic potential functions were defined in the simplest form.

2.2 Hill's yield function for anisotropic sheets under plane strain conditions

2.2.1 Analysis of air-bending of anisotropic sheet metal

The schematic diagram of sheet metal under pure bending is shown in Fig. 1. The following assumptions are applied: (1) the sheet is long enough relative to its

thickness. Therefore the strain in rolling direction (long direction) (x direction in Fig. 1) is zero; (2) Straight lines-perpendicular to the neural surface remain straight during the air-bending process; (3) Hill's theory of plastic anisotropy is adopted to describe the anisotropic characteristics of the sheet metal; (4) volume conservation is kept during air-bending process.

According to the above assumptions, the radius of neutral surface can be defined as: $r_n = r + t/2$ (see Fig. 1).

The distribution of transverse strain through thickness is:

$$\varepsilon_{yy} = \begin{cases} \dfrac{\rho - r_n}{r_n} = \dfrac{\rho - r - t/2}{r + t/2} & |\rho - r - t/2| < d; \\ \ln(\rho / r_n) = \ln(\dfrac{\rho}{r + t/2}) & |\rho - r - t/2| \geq d. \end{cases} \quad (16)$$

Where ε_{yy} is the transverse strain: ρ is the radius of the studied bending layer: d is half thickness of elastic region.

Elastic behavior according to Hooke's law can be written as follows for a state of plane strain:

$$\sigma_{yy} = E'\varepsilon_{yy} \quad \text{with} \quad E' = \frac{E}{1-\nu^2} \quad \text{, that is}$$

$$\sigma_{yy} = \frac{E}{1-\nu^2}\varepsilon_{yy} \quad (17)$$

Where E is young's modulus, ν is Poisson's ratio.

As the stress-strain relationship for plastic deformation, Swift's equation (some times referred to as extended Ludwik-Nadai) is adopted there:

$$\sigma_{yy} = K'(\varepsilon_{yy} + \bar{\varepsilon}_0)^2 \quad \text{with } K' = K(\frac{4}{3})^{(n+1)/2} \quad (18)$$

Where K′ is constant in Ludwik-Nadai and Swift's equation; K is the strength coefficient; n is the strain-hardening exponent; $\bar{\varepsilon}_0$ is the initial strain.

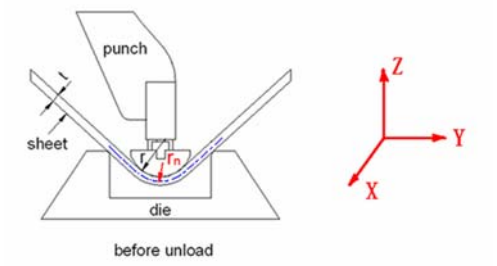

Fig. 1. Geometrical model of air-bending of sheet metal.

2.2.2 Solving for the distributions of stress and strain

According to Hill's quadratic yielding function, for anisotropic sheets, the material yields when

$$f(\sigma_{ij}, \varepsilon_{ij}) = \sigma_{xx}^2 + \sigma_{yy}^2 - \frac{2\bar{r}}{1+\bar{r}}\sigma_{xx}\sigma_{yy} + \frac{2}{1+\bar{r}}(\sigma_{zz}^2 - \sigma_{xx}\sigma_{zz} - \sigma_{yy}\sigma_{zz}) - \bar{\sigma}_e^2 = 0 \quad (19)$$

Under the plane strain condition, the plastic strain in rolling direction $\varepsilon_{xx} = 0$, so that:

$$d\varepsilon_{xx} = d\lambda \frac{\partial f(\sigma_{ij}, \varepsilon_{ij})}{\partial \sigma_{xx}} = 0 \quad (d\lambda \text{ is a coefficient}).$$

Combined with Eq.(19), $\bar{\sigma}_e$ can be expressed as:

$$\bar{\sigma}_e = \sqrt{1+2\bar{r}}\,|\sigma_{yy} - \sigma_{xx}| \quad (20)$$

$$\bar{\sigma}_e = \frac{\sqrt{1+2\bar{r}}}{1+\bar{r}}|\sigma_{yy} - \sigma_{zz}| \quad (21)$$

Based on plastic work formulation, the equivalent strain can be written as:

$$\bar{\varepsilon}_e = \frac{1+\bar{r}}{\sqrt{1+2\bar{r}}}|\varepsilon_{yy}| \quad (22)$$

From exponential strain hardening law, the relationship between the equivalent stress and equivalent strain is expressed as:

$$\bar{\sigma}_e = K(\bar{\varepsilon}_0 + \bar{\varepsilon}_e)^n \quad (23)$$

Where $\bar{\varepsilon}_0$ is the initial strain, $\bar{\varepsilon}_e$ is equivalent strain.

Substitution of Eq.(16) into Eq.(17) and Eq.(18) yields the distribution of σ_{yy}. Substitute Eq.(22) and Eq.(23) into Eq.(20) and Eq.(21), the distributions of σ_{xx}, σ_{zz}, σ_e, ε_{yy} and ε_e are solved, which are theoretical basis of numerical simulation used for air-bending forming of anisotropic sheet metal.

3. FE simulation for air-bending forming of anisotropic sheets

3.1 simulation algorithm

The FE simulation is done by ABAQUS/Explicit &standard solver. Due to the result of any time during the ABAQUS/Explicit module running can be treated as initial condition run in the ABAQUS/standard module for further calculating and analyzing, and vice versa. Therefore, ABAQUS function is very suitable for multi-step air-bending process: the explicit algorithm of ABAQUS/Explicit module fitted for dynamic and non-linear analysis could be used to simulate the sheet

metal forming process, and the implicit algorithm of ABAQUS/standard module adapted to static and steady analysis to simulate the springback process [20].

3.2 Simulation setup

The air-bending punch pressing speed of 8mm/s is chosen according to the operating requirements of URSVKEN 2200-ton press brake, and the mass scaling factor is set as 10. The plane stress element CPS8R and the plane strain element CPE8R are respectively applied to model the sheet and seven integration points are used through thickness to thoroughly simulate the sheet metal forming of single-step air-bending and multi-step air-bending. Anisotropic material model based on the hypothesis of plane stress and plane strain is implemented into a user-defined material subroutine for the finite element code ABAQUS. The punch and die are modeled as rigid surfaces. Coulomb's friction law is applied with a friction coefficient of 0.12 between the sheet, and the punch and die. The contact condition is implemented through a pure Master-slave contact-searching algorithm and penalty contact force algorithm. Finally, the explicit-implicit scheme is used for forming and springback stages respectively. To facilitate analysis, the 3D ABAQUS finite-element model is established for the process, as shown in Fig. 2.

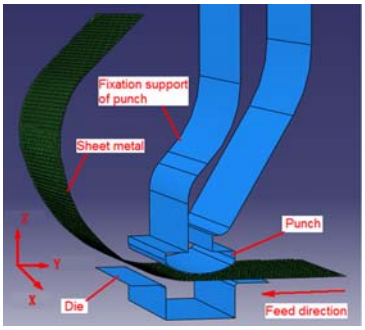

Fig. 2. Finite-element model of incremental air-bending forming process.

3.3 Simulation results and discussion

Single-step and multiple-step air-bending forming processes were simulated using the anisotropic material constitutive function under the conditions of plane stress and plane strain incorporated into ABAQUS. The single-step air-bending forming process was simulated to predict springback and the thickness strain distribution along the transverse direction. The multiple-step air-bending forming processes were simulated to predict the workpiece profile and assess the simulation effects with two constitutive models.

3.3.1 Single-step air-bending forming

The single-step air-bending tests were performed with WELDOX700, WELDOX900 and OPTIM960 anisotropic sheets. The material characteristic coefficients for these sheets were given in Table 1.

Table 1. Material properties.

Material	E(Mpa)	σ (Mpa)	n	ν	K(Mpa)	$\bar{r}$	Density(kg/m^3)
WELDOX7001	78846.66	99.8420.	0425	0.243	20.452	r0=0.79,r45=1.23,r90=0.96	7830
WELDOX900	205856.3	950.812	0.0385	0.284	22.331	r0=0.83, r45=1.15, r90=0.92	7830
OPTIM 960	204620	1257.59	0.0255	0.276	23.673	r0=0.96, r45=1.09, r90=0.89	7830

(E: Young's modulus, σ : Yield strength, n: Strain hardening exponent, ν : Poisson's ratio, k: Strength coefficient, $\bar{r}$: Anisotropy coefficient)

The single-step air-bending forming was simulated using two different material models: Hill 48 yield model under plane stress and Hill 48 yield model under plane strain.

In Fig. 3, the measured and predicted springback angles are compared. Based on this figure, the springback angle predicted by Hill 48 yield model under plane strain is nearly identical to the experimental values. Therefore, Hill 48 yield model based on the hypothesis of plane strain is capable of better prediction for springback of the anisotropic sheet metal.

Fig. 4 shows the comparison of the experimental and

predicted thickness strain along the transverse direction. It can be seen that the results predicted with Hill 48 yield model under plane strain are in much better agreement with experimental data than those predicted with Hill 48 yield model under plane stress. Obviously, Hill 48 yield model based on the hypothesis of plane strain is better able to predict thickness strain of the anisotropic sheets.

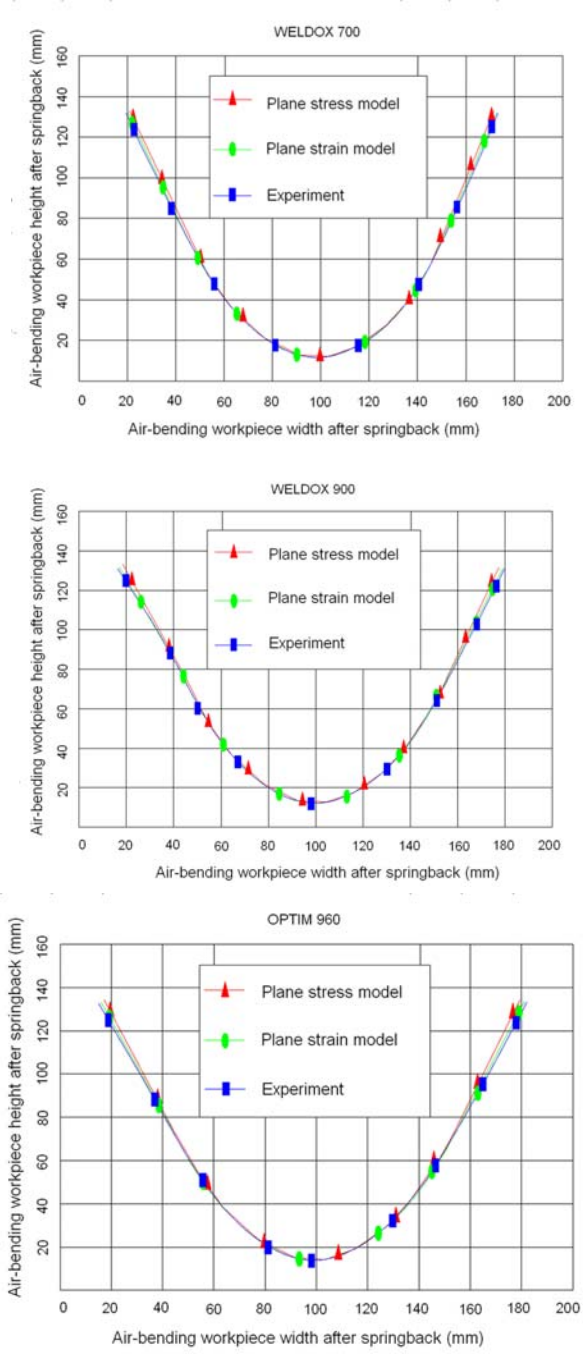

Fig. 3. Comparison of the experimental springback and the springback predicted with the plane strain and plane stress models for air-bending forming of WELDOX 700, WELDOX 900 and OPTIM 960 steel sheets.

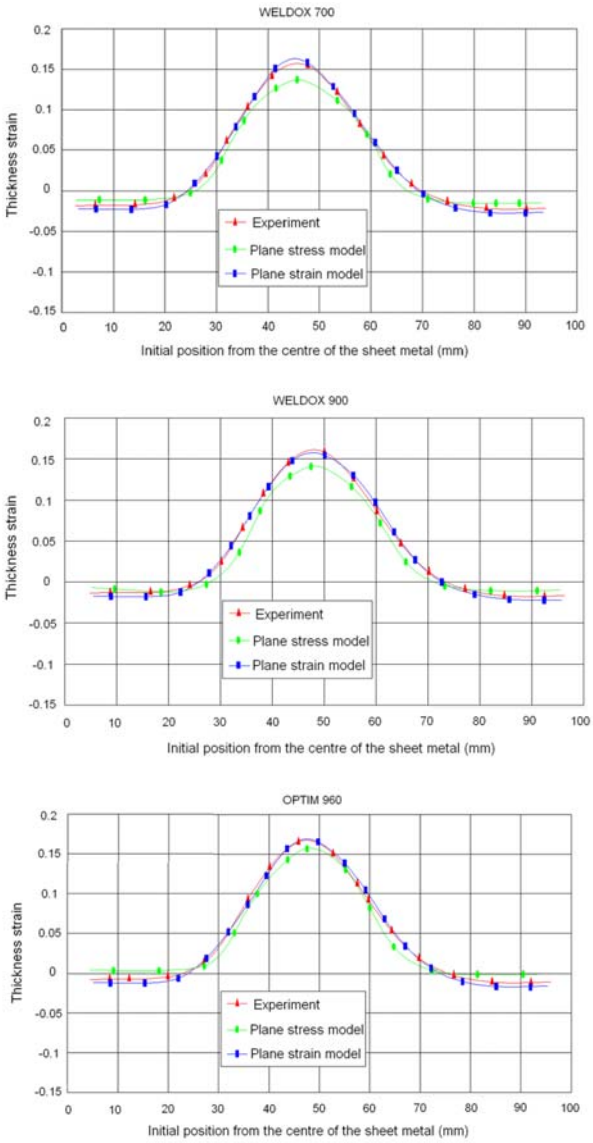

Fig. 4. Comparison of the experimental and predicted thickness strain along the transverse direction with Hill's anisotropic material model under the conditions of plane strain and plane stress.

3.3.2 Multiple-step incremental air-bending forming for semiellipse-shaped workpiece

The condition of multiple-step incremental forming is the same as the above single-step forming's. A comparison between the experimental part profiles with those obtained by simulation is shown in Fig. 5. As can be seen from the figures, the part profiles predicted by Hill 48 yield model under plane strain are very close to the actual experimental part profiles. Moreover, the relative errors of shape obtained with Hill 48 yield under plane strain are much lower than those obtained by Hill 48 yield mode under

plane stress. Therefore, Hill 48 yield model based on the hypothesis of plane strain has more accurate prediction ability. Hereby, we attempt to solve the key process parameters for multiple-step incremental air-bending forming of anisotropic sheet metal with the established Hill 48 yield model under plane strain.

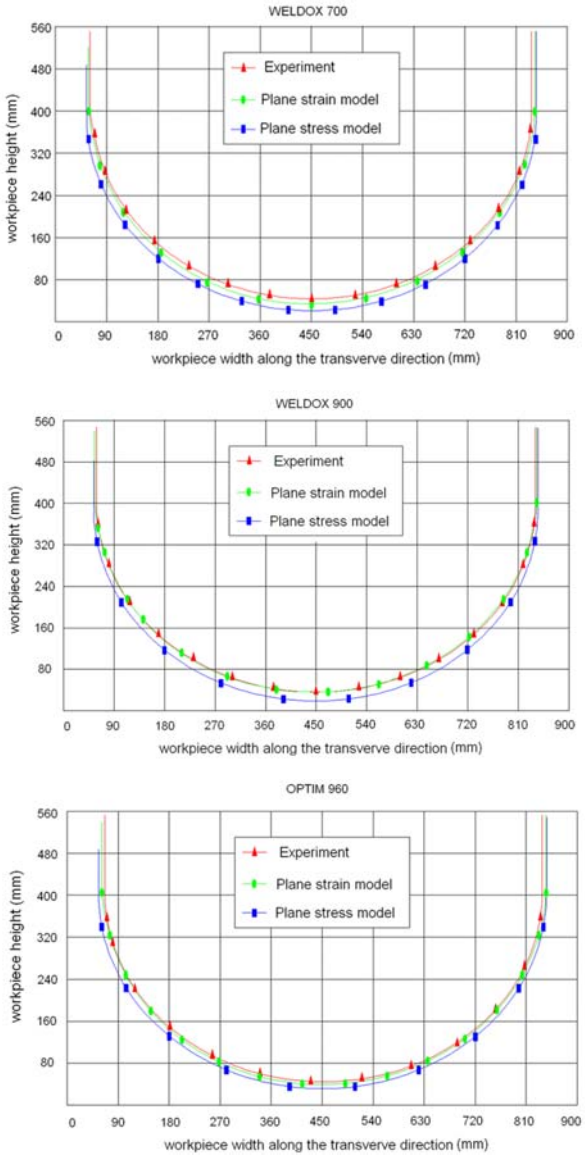

Fig. 5. Comparison of the target curve in the semiellipse-shaped workpiece neutral layer and the results predicted with the plane strain and plane stress models.

4. Application example

A semiellipse-shaped workpiece (Fig. 6) is formed at the URSVIKEN 2200-ton press brake with the process data obtained by Hill48 yield model under plane strain.

The surface profile of the workpiece is measured with Atos-II three dimensional laser measuring system, and a 3D point cloud model is obtained. The 3D point cloud model is matched with CAD model with Geomagic Qualify software, and the results show that the average dimension errors of the part are +0.573/−0.493 (Fig. 7), which meets the requirements of workpiece form and position accuracy.

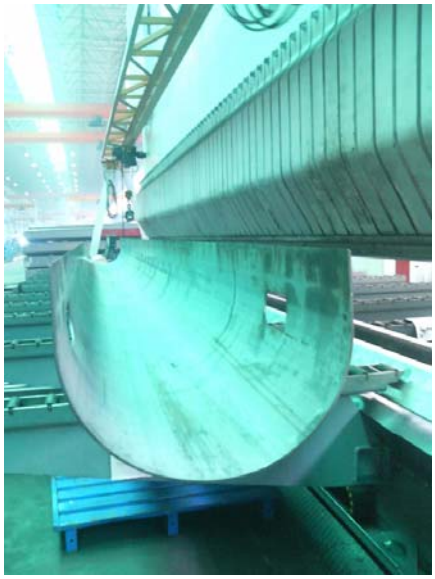

Fig. 6. The semiellipse-shaped hoist boom formed at the URSVKEN 2200-ton press brake.

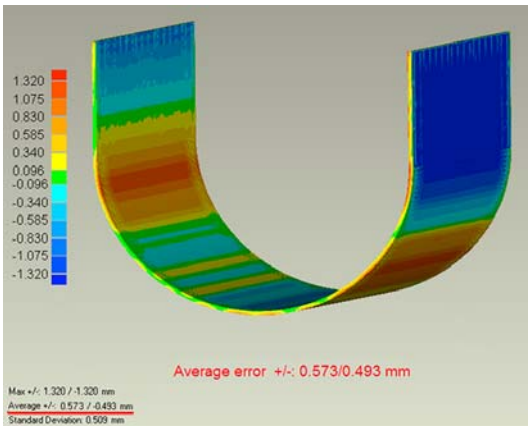

Fig. 7. Matching result of measured point cloud model of the cut one with 500 mm length from the scanned part and CAD model.

5. Conclusions

In this paper, material constitutive models based on Hill's yielding criterion under plane stress and plane strain conditions are developed. And the explicit expressions of elasto-plastic constitutive equation based on Hill

anisotropic yield criterion are implemented to ABAQUS software as the user subroutines. On the basis of the above, the finite element (FE) simulation is done by ABAQUS/Explicit & Standard solvers.

Under plane stress and plane strain conditions, ABAQUS finite-element models (FEM) are established for investigating single-step air-bending forming and multi-step incremental air-bending forming processes; and these processes are simulated with the FEM. In order to assess its ability to predict springback behaviors, Predictions of profile after springback and thickness strain along the transverse direction are evaluated by comparison with the experimental data and the simulation value. The results show that predictions by using plane strain anisotropic material model are much closer to the experimental values than those predicted with plane stress anisotropic material model. Moreover, the simulating and manufacturing results show that FEM simulation prediction method for multiple-step incremental air-bending forming of sheet metal with plane strain anisotropic material model is reasonable and effective. It can provide optimum processing parameters for incremental air-bending forming, which was successfully applied in manufacturing of one semiellipse-shaped workpiece used in crane boom.

Acknowledgements

This work was supported by Shanghai Institute of Technology Scientific Research Project of Talent Introduction, under YJ 2011-20; Shanghai Leading Academic Discipline Project, under J51501; and the National Nature Science Fund of People's Republic of China, under 51105256/E050301.

References

[1] Z. M. Fu, J. H. Mo, P. Gong, W. X. Zhang, Z. W. Li, K. Huang, International Journal of Mechanical Sciences, **51**, 732 (2009).
[2] R. Hill, P roc. R. Soc. Lond. A; **193**, 281 (1948).
[3] R. Hill, Clarendon Press. Oxford, 1950.
[4] R. Hill, Math. Proc. Cambridge Phil. Soc; **55**, 179 (1979).
[5] R. Hill, J. Mech. Phys. Solids, **38**, 405 (1990).
[6] R. Hill, Int. J. Mech. Sci, **35**, 19 (1993).
[7] F. Barlat, J. Lian, Int J Plasticity, **5**, 51 (1989).
[8] F. Barlat, D. J. Lege, J. C. Brem, Int. J. Plasticity, **7**, 693 (1991).
[9] F. Barlat, R. C. Becker, Y. Hayashida, Y. Maeda, Y. Yanagawa, K. Chung, J. C. Brem, D. J. Lege, K. Matsui, S. J. Murtha, S. Hattori, Int. J. Plasticity, **13**, 385 (1997).
[10] F. Barlat, Y. Maeda, K. Chung, M. Yanagawa, J. C. Brem, Y. Hayashida, D. J. Lege, K. Matsui, S. J. Murtha, S. Hattori, R. C. Becker, S. Makosey, J. Mech. Phys. Solids, **45**, 1727 (1997).
[11] F. Barlat, J. C. Brem, J. W. Yoon, K. Chung, R. E. Dick, D. J. Lege, F. Pourboghrat, S. H. Choi, E. Chu, Int. J. Plasticity; **19**, 1297 (2003).
[12] A. P. Karafillis, M. Boyce, J. Mech. Phys. Solids, **41**, 1859 (1993).
[13] F. S. Ming, Z. Li, SAE Technical Paper, 01, 1002 (1999).
[14] M. Gotoh, Int. J. Mech. Sci. **19**, 505 (1977).
[15] M. Gotoh, Int. J. Mech. Sci. **19**, 513 (1977).
[16] D. Banabic, T. Kuwabara, T. Balan, D. S. Comsa, D. Julean, International Journal of Mechanical Sciences, **45**, 797 (2003).
[17] J. H. Hahm, K. H. Kim, International Journal of Plasticity, **24**, 1097 (2008).
[18] J. W. Yoon, F. Barlat, R. E. Dick, K. Chung, T. J. Kang, International Journal of Plasticity, **20**, 495 (2004).
[19] W. Tong, International Journal of Plasticity, **22**, 497 (2006).
[20] Z. M. Fu, J. H. Mo, L. Chen, W. Chen, Materials and Design, **31**, 267 (2010).

*Corresponding author: wsmsuccess@163.com